NASA TECHNICAL MEMORANDUM

NASA TM X-52103

NASA TM X-52103

FILM BOILING HEAT TRANSFER TO WATER DROPS ON A FLAT PLATE

by Kenneth J. Baumeister, Thomas D. Hamill, F. L. Schwartz, and Glen J. Schoessow
Lewis Research Center
Cleveland, Ohio

TECHNICAL PREPRINT prepared for Eighth National Heat Transfer Conference sponsored by the American Society of Mechanical Engineers and the American Institute of Chemical Engineers
Los Angeles, California, August 8-11, 1965

NATIONAL AERONAUTICS AND SPACE ADMINISTRATION · WASHINGTON, D.C. · 1965

FILM BOILING HEAT TRANSFER TO WATER DROPS ON A FLAT PLATE

by Kenneth J. Baumeister, Thomas D. Hamill
F. L. Schwartz, and Glen J. Schoessow

Lewis Research Center
Cleveland, Ohio

TECHNICAL PREPRINT prepared for
Eighth National Heat Transfer Conference
sponsored by the American Society of Mechanical Engineers
and the American Institute of Chemical Engineers
Los Angeles, California, August 8-11, 1965

NATIONAL AERONAUTICS AND SPACE ADMINISTRATION

FILM BOILING HEAT TRANSFER TO WATER

DROPS ON A FLAT PLATE

by Kenneth J. Baumeister,* Thomas D. Hamill,*
F. L. Schwartz,** and Glen J. Schoessow***

ABSTRACT

The mass evaporation rates and overall heat transfer coefficients are determined both theoretically and experimentally for water drops which are supported by their own superheated vapor over a flat hot plate. The theoretical and experimental mass evaporation rates are found to agree within 20 percent for drop volumes from 0.05 to 1 cc and for plate temperatures from 600° to 1000° F. In this parameter range, the mass evaporation rate varies from 0.001 to 0.01 g/sec, the overall heat-transfer coefficient ranges between 40 and 70 Btu/(hr)(sq ft)(°F), and the theoretical gap thickness beneath the drop ranges between 0.003 and 0.008 in.

The water drops are assumed to have a flat disk geometry with a uniform vapor gap beneath the drop and a saturated steam vapor cover. The assumptions are made that the bottom of the drop is at the saturation temperature and that evaporation takes place uniformly beneath the drop with negligible energy dissipation.

For steady-state laminar incompressible flow, assuming constant properties, the exact Navier-Stokes equations, the continuity equation, and the energy equation are solved simultaneously to obtain the evaporation rate in terms of the drop volume, plate temperature, plate emissivity, and gravitational potential.

In addition, for the special case where radiation can be neglected, the heat-transfer coefficient is shown to be equal to

$$h_i = 0.68\left(\frac{k^3 \lambda_i^* g \rho_D P}{\Delta T\, \mu L_e}\right)^{1/4}$$

For heat transfer to the drop,

$$\lambda_D^* = \lambda\left(1 - \frac{c_p\, \Delta T}{\lambda}\right)$$

For heat transfer from the plate,

$$\lambda_p^* = \lambda\left(1 + 0.5\, \frac{c_p\, \Delta T}{\lambda}\right)$$

*Lewis Research Center, National Aeronautics and Space Administration, Cleveland, Ohio.

**Professor of Mechanical Engineering at University of Florida.

***Professor of Nuclear Engineering at University of Florida.

The difference in the two values of h results from the radial convection of the superheated vapor. The above equation for h is also shown to be useful up to drop volumes of 5 cc. Author

SYMBOLS

A	area, sq ft
a	constant of proportionality, sec^{-1}
c_p	specific heat of vapor, Btu/lb_m
F	axial pressure variable, sq ft
f	transformation variable, ft/sec
g	acceleration of gravity, ft/sec^2
g_c	dimensional conversion factor, 32.1739 $(ft)(lb_m)(lb_f^{-1})(sec^{-2})$
h	heat transfer coefficient, $Btu/(hr)(sq\ ft)(^oF)$
k	thermal conductivity, $Btu/(hr)(ft)(^oF)$
L_e	equivalent geometry factor, cm
l	average calculated drop thickness, cm
M	mass, g
N	surface tension, dyne/cm
P	static pressure, lb_f/sq ft gauge
q	rate of heat flow, Btu/hr
R	radius of curvature, cm
r_o	maximum radius of water disk, cm
T	temperature, ^oR
ΔT	$T_p - T_{sat}$
t	time, sec
U	overall heat-transfer coefficient, $Btu/(hr)(sq\ ft)(^oF)$
u	radial velocity, ft/sec
V	drop volume, cc

w axial velocity, ft/sec

y position of drop surface from prescribed reference surface, cm

α thermal diffusivity, sq ft/sec

β computer proportionality constant, V^{-1}

Γ material constant, $(in.)(sec^{-1})/(lb_f)(lb_m)^{-1/4}(cm^{1/2})(^oR^{-3/4})(cm^{-3/4})$

γ property constant, $ft^3/(lb_m)(^oR)$

δ steam gap thickness, in.

ϵ emissivity for radiation

ζ dimensionless coordinate

η property constant, $lb_m/(ft)(sec)(^oR)$

κ computer proportionality constant, V^{-1}

Λ sensible heat correction faction

λ latent heat of evaporation, Btu/lb_m

λ^* modified latent heat of evaporation, Btu/lb_m

μ absolute viscosity, $lb_m/(ft)(sec)$

ν kinematic viscosity, sq ft/sec

ρ density, lb_m/ft^3

σ computer proportionality constant, sec^{-1}

τ computer time, sec

υ specific volume, ft^3/lb_m

Φ computer transform variable, V

φ dimensionless transformation variable

Ψ computer transform variable, V

ψ dimensionless transformation variable

Ω material constant, $(g)(sec^{-1})(lb_m/lb_f)^{1/4}(cm^{1/2})(^oR^{-1/4})(cm^{-9/4})(V^{-1})$

Subscripts:

c convection

D drop

f film

i index

p plate

r radiation

sat evaluated at saturation condition

δ evaluated at lower surface of droplet

∞ asymptotic

Superscripts:

' derivative with respect to independent variable

. derivative with respect to τ

INTRODUCTION

The most recent and complete works on drop evaporation on a hot surface are by Gottfried (ref. 1) and Borishansky (ref. 2). Both authors presented dimensional and semi-empirical correlations for the evaporation of liquid drops in film boiling on a flat plate.

On the bases of Borishansky's experimental results and the experiments performed in conjunction with this paper, the general problem of water drop evaporation is broken down into the following states, which are governed by the volume of the drop: small spheroid, flat disk, and bubbly disk. These states are depicted in Figure 1.

In this particular study, water drops in the volume range 0.05 to 1 cc are analyzed. In this volume range, an analytical model based on a flat disk geometry, shown in Figure 2, reasonably satisfies the physical situation and yet still has simple enough boundary conditions to make the problem tractable.

METHOD OF ANALYSIS

General Approach

Consider the flat water drop model shown in Figure 2. Heat transfer to the drop takes place by convection and radiation through the superheated film. Heat transfer and evaporation from the upper surface are considered negligible in comparison to that beneath the drop (ref. 3).

The average drop thickness l and radius r_o have been determined analytically as a function of Vt. The analytical results compare favorably to experimental measurements by Borishansky (ref. 2). Physical observations indicate that the gap thickness δ is a function of radial position; however, to make the problem mathematically tractable, a uniform gap thickness δ is assumed.

Gottfried (ref. 1) and Kutateladze (ref. 3) pointed out that the flow under consideration is well within the laminar range; thus, the flow is treated as incompressible with negligible energy dissipation. In addition, the drop at any instant is assumed to be in a steady-state condition. Consequently, for this case of axisymmetrical flow, the governing equations are as follows:

Momentum

$$u \frac{\partial u}{\partial r} + w \frac{\partial u}{\partial z} = - \frac{g_c}{\rho} \frac{\partial P}{\partial r} + \nu \left(\frac{\partial^2 u}{\partial r^2} + \frac{1}{r} \frac{\partial u}{\partial r} - \frac{u}{r^2} + \frac{\partial^2 u}{\partial z^2} \right) \tag{1}$$

$$u \frac{\partial w}{\partial r} + w \frac{\partial w}{\partial z} = - \frac{g_c}{\rho} \frac{\partial P}{\partial z} + \nu \left(\frac{\partial^2 w}{\partial r^2} + \frac{1}{r} \frac{\partial w}{\partial r} + \frac{\partial^2 w}{\partial z^2} \right) \tag{2}$$

Continuity

$$\frac{\partial u}{\partial r} + \frac{u}{r} + \frac{\partial w}{\partial z} = 0 \tag{3}$$

Energy:

$$u \frac{\partial T}{\partial r} + w \frac{\partial T}{\partial z} = \alpha \nabla^2 T \tag{4}$$

---

†The equilibrium equation

$$\frac{1}{R_1} + \frac{1}{R_2} = \frac{\rho_D (g/g_c) y}{N}$$

was solved numerically for the drop shape in reference 4.

The boundary conditions for equations (1) to (4) are

$$z = 0 \qquad u = 0 \qquad w = 0 \qquad T = T_p \tag{5}$$

$$z = \delta \qquad u = 0 \qquad w = w(\delta) \qquad T = T_{sat} \tag{6}$$

Static equilibrium (neglecting axial momentum change, see ref. 4):

$$\int_0^{r_o} P(r,\delta)2\pi r \, dr = V\rho_D \frac{g}{g_c} \tag{7}$$

Interface energy balance:

$$\lambda \frac{dM}{dt} = q_c + q_r \tag{8}$$

The assumptions are made that the bottom of the drop is at the saturation temperature and that the evaporation takes place uniformly beneath the drop.

In performing the analysis, the following calculational procedure is used. A gap thickness δ is assumed. Then the evaporation rate required to satisfy the static equilibrium condition (eq. (7)) is found by solution of the momentum equations. However, for the same assumed gap thickness δ the evaporation rate from the surface of the drop can be determined from energy considerations. In general, for the first assumed value of the gap thickness δ, the mass evaporation rate calculated from momentum considerations will not be equal to the mass evaporation rate calculated from energy considerations. Therefore, some type of iteration on the gap thickness δ is required in order to bring the calculated momentum and energy evaporation rates into balance. In this paper, the iteration is performed by combining the solutions of the momentum and energy equations in a graphical manner to determine the unique value of the gap thickness δ, which will permit all the governing equations and boundary conditions to be satisfied concurrently. Further details in the analytical treatment follow.

In addition, for the special case where radiation is negligible, the heat-transfer coefficients are derived analytically in closed form.

Momentum Equations

Assuming constant fluid properties, the interaction between the equation of motion with the energy equation ceases, and the velocity field no longer depends on temperature. The properties of the flow field are evaluated at the film temperature, defined as,

$$T_f = \frac{T_p + T_{sat}}{2} \tag{9}$$

Use of the method of similarity at this time reduced the partial equations (1) to (3) into a set of ordinary nonlinear differential equations. The similarity transforms used in the problems of three-dimensional axisymmetric stagnation flow (ref. 5) will suffice. They are

$$w = -2f(z) \tag{10}$$

$$u = rf'(z) \tag{11}$$

$$P = \frac{1}{2} a^2 \frac{\rho}{g_c} \left[r_o^2 - r^2 + F(z) \right] \tag{12}$$

Performing the transformation results in the ordinary equations

$$f'^2 - 2ff'' = a^2 + \nu f''' \tag{13}$$

$$2ff' = -\frac{1}{4} a^2 F' - \nu f'' \tag{14}$$

Equations (13) and (14) can be nondimensionalized by using the following transformations:

$$\zeta = \sqrt{\frac{a}{\nu}}\, z \tag{15}$$

$$f(z) = \sqrt{a\nu}\, \varphi(\zeta) \tag{16}$$

$$F(z) = \frac{4\nu}{a} \psi(\zeta) \tag{17}$$

The governing momentum equations take on the form

$$\varphi'^2 - 2\varphi\varphi'' = 1 + \varphi''' \tag{18}$$

$$2\varphi\varphi' = -\psi' - \varphi'' \tag{19}$$

The boundary conditions (5) and (6) become

$$\zeta = 0 \qquad \varphi = 0 \qquad \varphi' = 0 \qquad \psi = 0 \qquad T = T_p \tag{20}$$

$$\zeta = \sqrt{\frac{a}{\nu}}\, \delta \qquad \varphi = \frac{-w(\delta)}{2\sqrt{a\nu}} \qquad \varphi' = 0 \qquad T = T_{sat} \tag{21}$$

The method of solution is to first assume many reasonable values of δ and to solve for the flow distribution in each of these cases that satisfy the static equilibrium condition (eq. (7)).

The solution of equations (18) and (19) in this particular situation is easily performed by means of an analog computer. However, instead of assuming values of δ, initial values of φ'' are assumed.

Analog Solution of Momentum Equations

The first step in programing equations (18) and (19) for the analog computer is to change the variables to computer variables by making the following transformations:

$$\zeta = \sigma\tau \tag{22}$$

$$\varphi(\zeta) = \kappa\Phi(\tau) \tag{23}$$

$$\psi(\zeta) = \beta\Psi(\tau) \tag{24}$$

where the symbols σ, κ, β are constant scale factors. The symbol τ represents the computer time: the time for the phenomena to occur in the computer. The distance from the plate is directly related to the computer time τ.

Substituting equations (22) to (24) into equations (18) and (19) results in the analog momentum equations

$$\dddot{\Phi} = \kappa\sigma\dot{\Phi}^2 - 2\kappa\sigma\Phi\ddot{\Phi} - \frac{\sigma^3}{\kappa} \tag{25}$$

$$\dot{\Psi} = -2\frac{\kappa^2}{\beta}\Phi\dot{\Phi} - \frac{\kappa}{\beta\sigma}\ddot{\Phi} \tag{26}$$

The boundary conditions on equations (25) and (26) take on the form

$$\tau = 0 \qquad \Phi = 0 \qquad \dot{\Phi} = 0 \qquad \psi = 0 \qquad T = T_p \tag{27}$$

$$\tau = \frac{1}{\sigma}\sqrt{\frac{a}{\nu}}\,\delta \qquad \Phi = -\frac{1}{\kappa}\frac{w(\delta)}{2\sqrt{a\nu}} \qquad \dot{\Phi} = 0 \qquad T = T_{sat} \tag{28}$$

Equations (25) and (26) are programed for the analog computer for values of $\sigma = 1$, $\kappa = 1$, and $\beta = 1$, which imply for this first program that $\zeta = \tau$, $\varphi = \Phi$, and $\psi = \Psi$.

Figure 3 represents the solution for φ'. The set of discrete initial conditions on φ'' is selected over a sufficiently wide range to give a reasonable topology of the total set of solutions to this particular initial value problem. The requirement of satisfying the boundary conditions on φ' limits the acceptable range of $\varphi''(0)$ to

$$0 < \varphi''(0) < 1.31 \tag{29}$$

Trial and error procedure indicates that for the range of interest; scale factors of $\sigma = 0.1$, $\kappa = 0.001$, and $\beta = 0.0015$ can be used. Rescaling is necessary to reduce the error in the analog output. The program results are shown in Figures 4, 5, and 6, which represent $\dot{\Phi}$, Φ, and Ψ, respectively.

The results are as expected. The parameter $\dot{\Phi}$, which for a fixed r is directly related to u, starts at 0, goes to a maximum value near the center of the gap, and then returns to zero at the surface of the drop. The parameter Φ, which is directly related to w, starts at zero at the plate and then reaches its maximum value at the bottom of the drop. The parameter Ψ, which is directly related to the static pressure, goes from a maximum value of zero at the plate to a minimum value in the center of the channel, because the static pressure head at the plate is partially converted into a velocity head in the center of the gap. The pressure then returns nearly to its plate value at the surface of the drop. Therefore, the pressure distribution at the surface of the drop is taken to be of the form

$$P(r,\delta) \cong \frac{1}{2} a^2 \frac{\rho}{g_c} (r_o^2 - r^2) \tag{30}$$

Table I lists the important numerical values of the end points of Figures 4 and 5.

Velocities and Mass Flow Rate

The radial and axial velocities and the gap thickness are determined from the analog parameters listed in Table I. These parameters are directly related to the axial velocity w by equations (10), (16), and (23) resulting in

$$w = - 2 \sqrt{a\nu} \; \kappa\Phi \tag{31}$$

The value of w at the surface of the drop is given by

$$w(\delta) = - 2 \sqrt{a\nu} \; \kappa\Phi_\delta \tag{32}$$

where Φ_δ is the value of Φ at the surface of the drop.

In a similar manner, the time required to satisfy the boundary condition of $\dot{\Phi} = 0$ relates directly to the gap thickness δ by equations (15) and (22), resulting in

$$\delta = \sqrt{\frac{\nu}{a}} \, \sigma\tau_\delta \tag{33}$$

The parameter a is now determined by substituting equation (30) into equation (7), noting that for a flat disk geometry,

$$V = A \times l = \pi r_o^2 l \tag{34}$$

results in

$$a = \sqrt{4\Pi g_c}\ (g/g_c)^{1/2}\left(\frac{\rho_D}{\rho}\right)^{1/2} l\left(\frac{1}{V}\right)^{1/2} \tag{35}$$

The mass loss from the drop is

$$\frac{dM}{dt} = \rho\left|w(\delta)\right| A \tag{36}$$

For steam the specific volume and absolute viscosity may be expressed as

$$\upsilon = \gamma T_f \qquad \mu = \eta T_f \tag{37}$$

Substituting equations (32), (35), and (37) into equation (36) results in

$$\frac{dM}{dt} = \Omega(g/g_c)^{1/4}\ l^{-1/2}\ T_f^{1/4}\ V^{3/4}\ \Phi_\delta \tag{38}$$

where

$$\Omega = 64\Pi g_c\rho_D)^{1/4}\ \kappa\left(\frac{\eta^2}{\gamma}\right)^{1/4} \tag{39}$$

Equation (38) is to be evaluated for different values of the gap thickness. Substituting equations (35) and (37) into equation (33) results in the following relation for the gap thickness:

$$\delta = \Gamma\tau_\delta(g/g_c)^{-1/4}\ l^{-1/2}T_f^{3/4}\ V^{1/4} \tag{40}$$

where

$$\Gamma = \frac{\sigma(\gamma\eta^2)^{1/4}}{(4\Pi g_c\rho_D)^{1/4}} \tag{41}$$

Energy Equation

For the problem under consideration, the physical conditions indicate that

$$u\frac{\partial T}{\partial r} << w\frac{\partial T}{\partial z} \tag{42}$$

Therefore, transforming equation (4) to computer variables, assuming

$$\Phi \cong \frac{\Phi_\delta}{\tau_\delta}\tau \tag{43}$$

and integrating result in

$$T = C_4 \frac{1}{2}\left[\sqrt{\frac{2\Pi}{B}}\ \mathrm{erf}\left(\sqrt{\frac{B}{2}}\ \tau\right)\right] + C_5 \tag{44}$$

where

$$B = \frac{2Pr\kappa\sigma\Phi_\delta}{\tau_\delta} \tag{45}$$

Expanding equation (44) in series form and defining

$$\Delta = \frac{B}{6}\ \tau_\delta^2 \tag{46}$$

neglecting second order terms, and evaluating the constants yield

$$T = T_p - \frac{(T_p - T_{sat})\tau}{(1 - \Delta)\tau_\delta}\left[1 - \Delta\left(\frac{\tau}{\tau_\delta}\right)^2\right] \tag{47}$$

The heat flux at the drop interface is found from the relation

$$q_c = - kA \left.\frac{dT}{dz}\right|_\delta = - \frac{kA}{\sigma}\sqrt{\frac{a}{\nu}} \left.\frac{dT}{d\tau}\right|_\delta \tag{48}$$

Differentiating relation (47) and substituting this result into equation (48) along with equation (33) yield

$$q_c = \frac{kA}{\delta}(T_p - T_{sat})\Lambda_D \tag{49}$$

where

$$\Lambda_D = \left(\frac{1 - 3\Delta}{1 - \Delta}\right) \cong (1 - 2\Delta) \tag{50}$$

The amount of mass transfer from the water drop is now calculated as a function of δ. The convection energy flux is represented by equation (49), while the radiative flux is given approximately by the relation

$$q_r = \epsilon_p A F_T (T_p - T_{sat}) \tag{51}$$

where

$$F_T = \frac{\sigma_o(T_p^4 - T_{sat})}{T_p - T_{sat}} \tag{52}$$

The absorption of some of the radiative energy by the water vapor is neglected in this problem because of the small path length between the drop and the plate. In addition, the emissivity of the water drop is assumed to be approximately unity. Substituting equations (49), (51), and (34) into equation (8) and solving for the evaporation rate yield

$$\frac{dM}{dt} = \frac{V}{l\lambda}\left(\frac{k\Lambda_D}{\delta} + \epsilon_p F_T\right)(T_p - T_{sat}) \tag{53}$$

with all the temperature dependent properties evaluated at the film temperature (eq. (9)).

The overall heat-transfer coefficient U between the plate and the water drop is defined by

$$U = \frac{\lambda \frac{dM}{dt}}{A(T_p - T_{sat})} \tag{54}$$

Graphical Determination of Gap Thickness and Evaporation Rate

The evaporation of water vapor from a water drop has been determined from momentum and energy transfer equations (eq. (38) and (53)) for various values of gap thickness as found from equation (40). The point of intersection of the momentum and energy equations in Figure 7 represents the conditions where all the governing equations and boundary conditions (1) to (8) are satisfied concurrently.

EXPERIMENTAL PROCEDURES

The evaporation rate is determined experimentally from measurements taken on the total vaporization time, that time required for the entire volume of liquid which is placed on a heating surface to vaporize completely. Plots of the experimental data for distilled water near the saturation temperature are shown in Figures 8 to 10. The slopes of the curves, rate of change of volume with respect to time, represent the evaporation rate of the drop.

The data shown in Figure 8 indicate quite plainly that the surface condition has no noticeable effect on the vaporization time. However, at higher plate temperatures a variation due to radiation effects is expected.

A slight problem with the flat heating surface resulted from the movement of the water drop against the barrier wall during the vaporization process. To eliminate the effect of contact with the barrier wall on the experimental evaporation rate, the experimental data to be used in comparison with the theoretical results were taken on a test section with a 1° apex angle. A complete description of the test section and instrumentation can be found in reference 4. Figure 9 presents a comparison of the total vaporization times as measured on a flat surface and a conical surface with a 1° apex angle. As seen in this figure, there is no noticeable difference in the vaporization times.

EVAPORATION RATES

The mass evaporation rate is determined from the slope of a curve $V = f(t)$ prescribed by a set of tabulated values (V_i, t_i). The slope of the 1^o apex plate data is determined by differentiating a third-order polynomial fit of the total vaporization time data. The polynomial is of the form

$$V = P(1)t + P(2)t^2 + P(3)t^3 \tag{55}$$

where t is the time required to completely vaporize a drop of initial volume V. The coefficients in equation (55) are listed in Table II as a function of the plate temperature. They were determined by minimizing the weighted squares of the residuals. Weights of V^{-1} were used.

The curves shown in Figure 10 are drawn from equation (65) using the coefficients listed in Table II. Thus, the experimental evaporation rate equals

$$\frac{dM}{dt} = \rho_D \left[P(1) + 2P(2)t + 3P(3)t^2 \right] \tag{56}$$

The theoretical and experimental results are shown jointly in Figure 11. The emissivities chosen in the theoretical calculations are based on data tabulated in reference 6. As seen in Figure 11, agreement exists throughout the volume and temperature range considered. The deviation of theory and experiment is less than 20 percent.

Deviation of the model from the actual physical geometry and drop oscillations which occur at temperatures above 800^o F could account for some of the deviation between theory and experiment.

The calculated gap thickness, as shown in Figure 12, is relatively insensitive to volume changes, but is affected by increased plate temperatures.

OVERALL HEAT-TRANSFER COEFFICIENT

The overall heat-transfer coefficients to the drop, shown in Figure 13, as defined by equation (54), are evaluated for various drop volumes and plate temperatures of 600^o and 1000^o F.

The amount of thermal radiation is calculated to be 2 Btu/(hr)(sq ft) at 600^o F and 4.4 Btu/(hr)(sq ft) at 1000^o F. Consequently, radiation heat transfer at 600^o F represents less than 5 percent of the overall heat-transfer coefficient; while at 1000^o F, it represents less than 10 percent. As the drop volume decreases, the percentage of radiative heat transfer decreases still further because of the relative increase of conduction heat transfer which results from the smaller gap thickness at the lower drop volumes.

Closed Solution for h

Since greater physical insight into the effect of the system parameters (fluid properties, gravity, geometry, and the temperature gradient) on the rate of heat transfer is always enhanced by obtaining a closed solution for the heat-transfer coefficient, an attempt was made to correlate the numerical solutions in terms of simple analytic expressions. This attempt was successful, leading ultimately to a simple expression for h. The method of attack is briefly outlined below.

The end points of Figure 5 define a solution locus for the hydrodynamic problem (shown by the dashed line.) This locus is a solution in the sense that it provides a parametric relation between the velocity at the interface and the gap thickness. A plot of this locus on log-log paper gives a straight line, the final equation being

$$\Phi_\delta = 0.086\ \tau_\delta^3 \tag{57}$$

Substituting equations (21) to (23) into equation (57) yields

$$-\,w(\delta) = 0.172\ \frac{a^2}{\nu}\ \delta^3 \tag{58}$$

In terms of physical variables, this equation states that the interface velocity is proportional to the cube of the gap thickness. Equation (58) is now combined with the heat-transfer solution (which also contains δ) with the ultimate aim of eliminating δ. If radiation is neglected, the heat balance at the interface becomes

$$-\,\rho\lambda w(\delta) = \frac{k\Lambda_D}{\delta}\,(T_w - T_s) \tag{59}$$

For the heat transfer to the drop, the sensible heat factor Λ_D is found by combining equations (50), (46), (45), and (28);

$$\Lambda_D = 1 + \frac{\ell}{3}\,\frac{P_r w(\delta)\delta}{\nu} \tag{60}$$

Combining equations (59) and (60) produces a simpler expression for Λ_D

$$\Lambda_D = \frac{1}{1 + \frac{1}{3}\,\frac{c_p\,\Delta T}{\lambda}} \tag{61}$$

Combining equations (58), (59), and (61) results in the heat-transfer coefficient to the drop of the form

$$h_i = \frac{k\Lambda}{\delta} = 0.68\left(\frac{k^3\lambda_i^* g\rho_D\,\rho}{\Delta T\ \mu L_e}\right)^{1/4} \tag{62}$$

where

$$L_e \equiv \frac{V}{\pi^2 l^2} \tag{63}$$

and an expression for a modified latent heat of evaporation

$$\lambda_D^* = \lambda \Lambda_D^3 = \frac{\lambda}{\left(1 + \frac{1}{3}\frac{c_p \Delta T}{\lambda}\right)^3} \cong \lambda \left(1 - \frac{c_p \Delta T}{\lambda}\right) \tag{64}$$

The values of L_e for a given drop volume are found in Figure 14 for water. The values of L_e were determined from the l values in reference 4.

The heat-transfer coefficient from the plate can be shown to be similar to equation (62) with the exception that Λ and λ take on the form

$$\Lambda_P = \frac{1}{1 - \Delta} \simeq 1 + \Delta \tag{65}$$

and

$$\lambda_P^* = \lambda \Lambda_P^3 = \frac{\lambda}{\left(1 - \frac{1}{6}\frac{c_p \Delta T}{\lambda}\right)^3} \simeq \lambda \left(1 + \frac{0.5\ c_p \Delta T}{\lambda}\right) \tag{66}$$

Equation (62) is identical in form to Bromley's equation (ref. 3) with the exception of the specially defined geometry factor L_e. The difference between the two expressions for the heat-transfer coefficients (heat transfer to the drop $i = D$; heat transfer from the plate $i = p$) is a result of sensible heating in the vapor layer.

Vaporization Times

In principle, the evaporation history of a drop can be computed by employing a quasi-steady-state heat-transfer approach. Mathematically this is expressed by

$$\rho_D \lambda \frac{dV}{dt} = h(v) A \Delta T \tag{67}$$

where both h and A vary with time as the drop evaporates. The drop area is in general a complicated function of volume; however, in the case of large drops, for example, water drops greater than 1 cc, the thickness of the drop becomes constant. In this case, equation (67) can be integrated in a simple manner. Thus, for large drops

$$A = V/l_\infty \tag{68}$$

$$h = CV^{-1/4} \tag{69}$$

where l_∞ is the asymptotic drop thickness and C is a constant for a given temperature difference. For large water drops at a plate temperature of 600° F,

equation (67) becomes

$$dV/dt = 0.059\ V^{3/4} \tag{70}$$

Integrating from a drop volume of 1 cc to some larger value gives

$$(V^{1/4} - 1) = 0.00148\ (t - t_1) \tag{71}$$

where $(t - t_1)$ is the time taken for a drop to decrease from volume V to 1 cc. This relation is tested in Figure 15 by comparison with experimental data. The linearity of the plot verifies the present theory although the slope of the experimental and theoretical lines differ by 27 percent. This deviation is expected since at large drop volumes some of the vapor escapes through the drop in the form of bubbles. This added path of vapor escape should result in smaller evaporation times than those predicted by theory, which proves true for this example.

CONCLUSIONS

The analytical model developed in this paper can be used to predict the evaporation rate and overall heat-transfer coefficient for water drops on a flat plate in the film boiling regime by a graphical method with a reasonable degree of accuracy over the range of parameters investigated. For the special case where radiation can be neglected, the heat-transfer coefficient is shown to be equal to

$$h_i = 0.68\left(\frac{k^3\lambda_i^* g\rho_D\rho}{\Delta T\ \mu L_e}\right)^{1/4}$$

For heat transfer to the drop

$$\lambda_D^* = \lambda\left(1 - \frac{c_p\ \Delta T}{\lambda}\right)$$

For heat transfer from the plate

$$\lambda_P^* = \lambda\left(1 + 0.5\ \frac{c_p\ \Delta T}{\lambda}\right)$$

The difference between the two values of h results from the radial convection of the superheated vapor.

Figure 14 can be used to directly determine the overall heat-transfer coefficient from the hot plate to the water drop. Also, the equations and the analog computer results (Figs. 3 to 6) can be applied to any fluid, since the momentum equations were solved in dimensionless form.

Finally, it is shown by correlation of volume as a function of vaporization time that the basic equation for the heat-transfer coefficient can also be applied to large drops for which the steam intermittently breaks through the surface.

REFERENCES

1. Gottfried, B. S.: The Evaporation of Small Drops on a Flat Plate in the Film Boiling Regime. Case Institute of Technology, Ph.D. Thesis, 1962.

2. Borishansky, V. M.: Heat Transfer to a Liquid Freely Flowing Over a Surface Heated to a Temperature Above the Boiling Point. Problems of Heat Transfer During a Change of State: A Collection of Articles. AEC-tr-3405, 1953.

3. Kutateladze, S. S.: Fundamentals of Heat Transfer. Academic Press, Inc., New York, 1963.

4. Baumeister, K. J.: Heat Transfer to Water Droplets on a Flat Plate in the Film Boiling Regime. Ph.D. Thesis, Univ. of Florida, 1964.

5. Schlichting, H.: Boundary Layer Theory. McGraw-Hill Book Company, Inc., New York, 1960.

6. McAdams, William H.: Heat Transmission. Third ed., McGraw-Hill Book Company, Inc., New York, 1954.

TABLE I. - ANALOG COMPUTER RESULTS

$\Phi(0)$, V	$\tau_\delta = \frac{1}{\sigma}\sqrt{\frac{a}{\nu}}\,\delta$, sec	$\Phi_\delta = -\frac{1}{2}\frac{w(\delta)}{K\sqrt{a\nu}}$, V	$\dot{\Phi}\left(\frac{\delta}{2}\right)$, V [a]
5.0	9.9	82.0	12.25
4.0	7.0	29.5	6.25
3.0	5.3	13.0	3.50
2.0	3.6	4.0	1.50

[a]The output of the analog computer is read in volts; however, the output $\dot{\Phi}$ is considered to be volts per unit time when used in the equations, in order that the units will be consistent.

TABLE II. - POLYNOMIAL COEFFICIENTS

Temperature of plate, ^{o}F	P(1)	P(2)	P(3)
608	$-7.2266.10^{-5}$	$+4.8950.10^{-6}$	$+4.4080.10^{-9}$
1014	$+4.0022.10^{-5}$	$+1.0295.10^{-5}$	$+5.4745.10^{-8}$

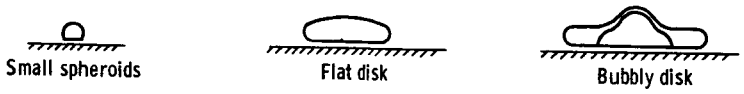

Figure 1. - Drop states.

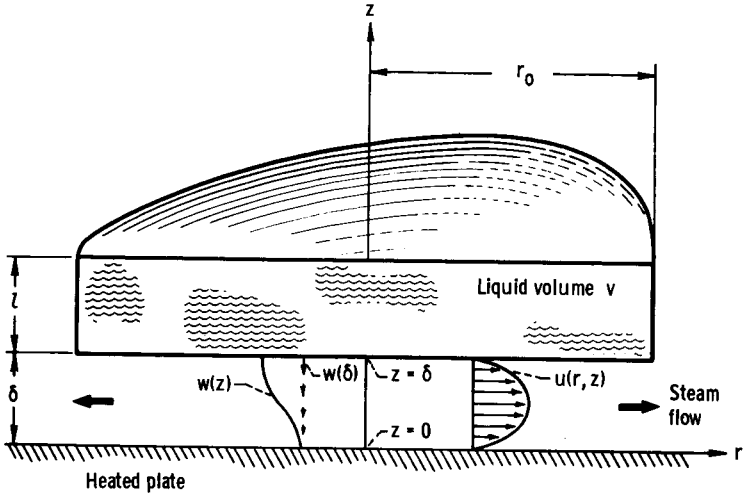

Figure 2. - Schematic model of the evaporation of a flat disk.

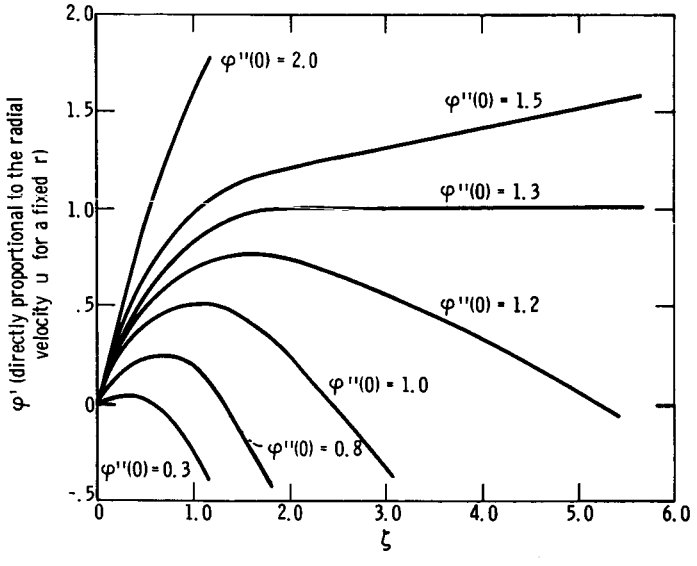

Figure 3. - φ' as a function of the assumed $\varphi''(0)$.

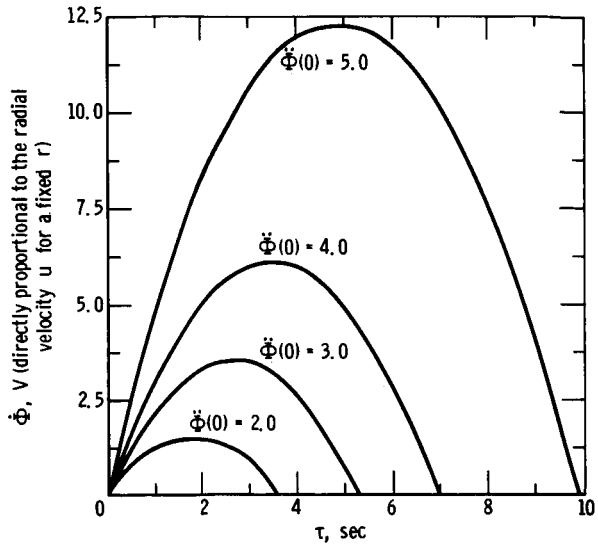

Figure 4. - $\dot{\Phi}$ as a function of the assumed $\ddot{\Phi}(0)$.

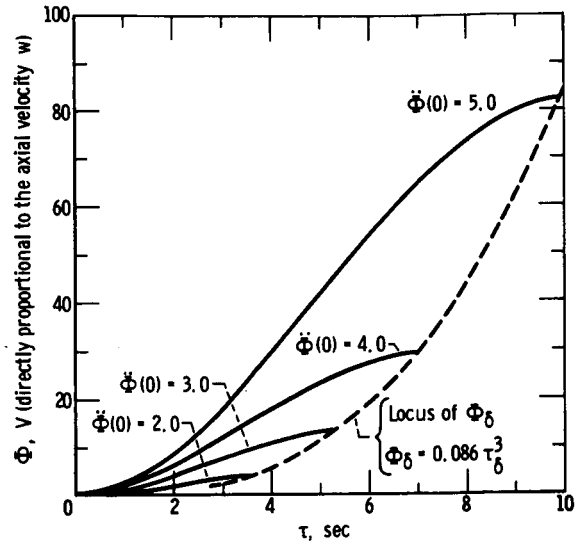

Figure 5. - Φ as a function of the assumed $\ddot{\Phi}(0)$.

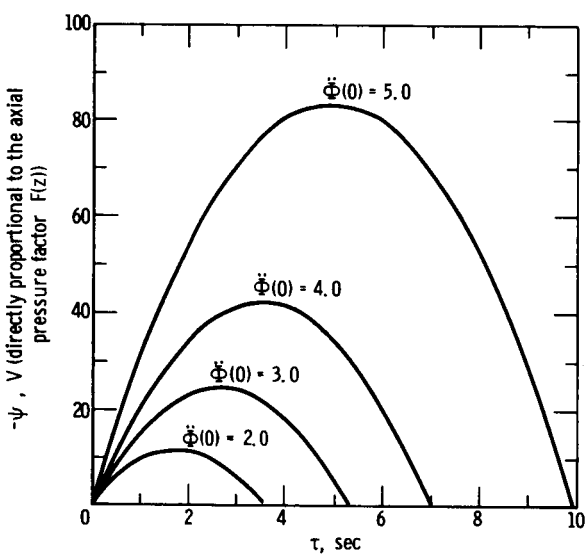

Figure 6. - ψ as a function of the assumed $\ddot{\Phi}(0)$.

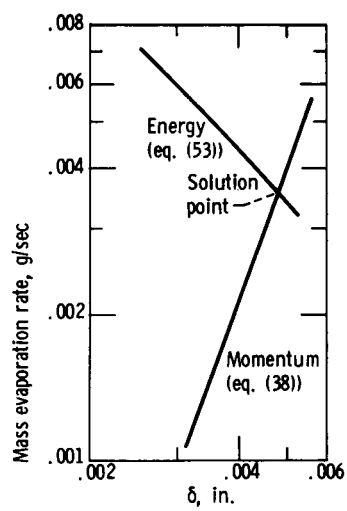

Figure 7. - Graphical simultaneous solution of momentum and energy equations at a droplet volume of 0.5 cc, a plate temperature of 600° F, and a plate emissivity of 0.5.

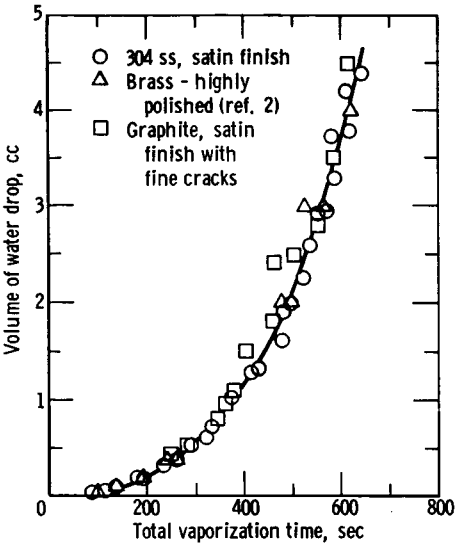

Figure 8. - Total vaporization time for water drops on a flat plate as a function of their volume for various surface conditions at a plate temperature of approximately 600° F.

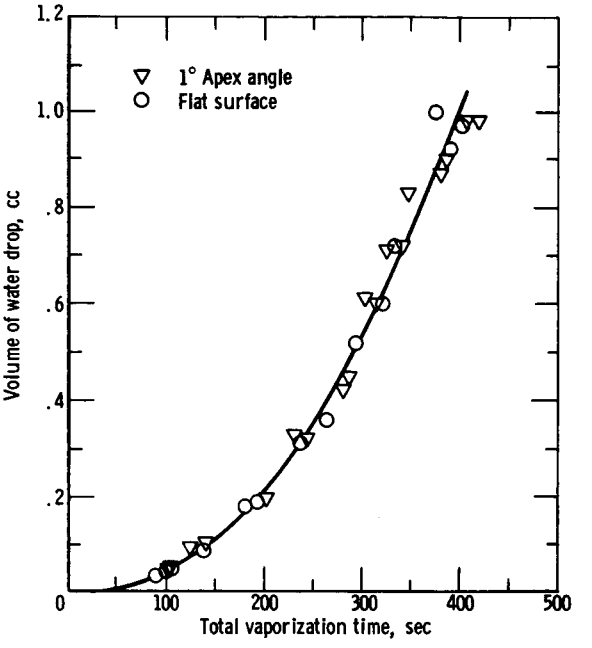

Figure 9. - Comparison of the total vaporization time for water drops on a flat plate and a 1° conical surface at approximately 600° F.

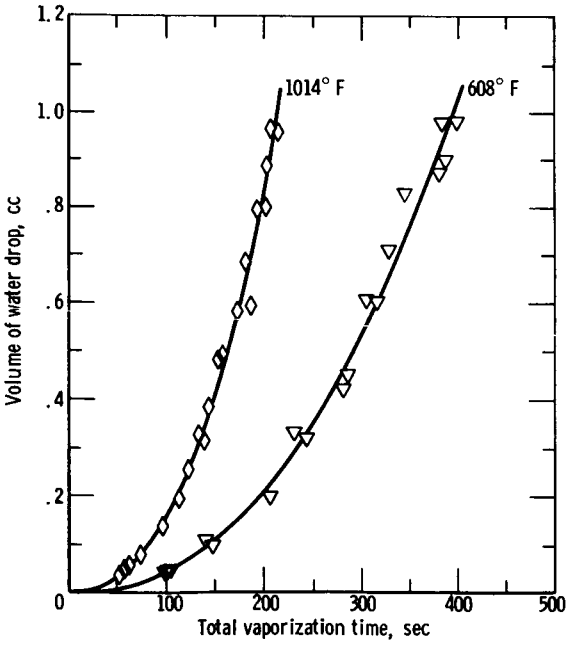

Figure 10. - Total vaporization time for water drops as a function of their volume and temperature of the heating surface which had a 1° apex angle.

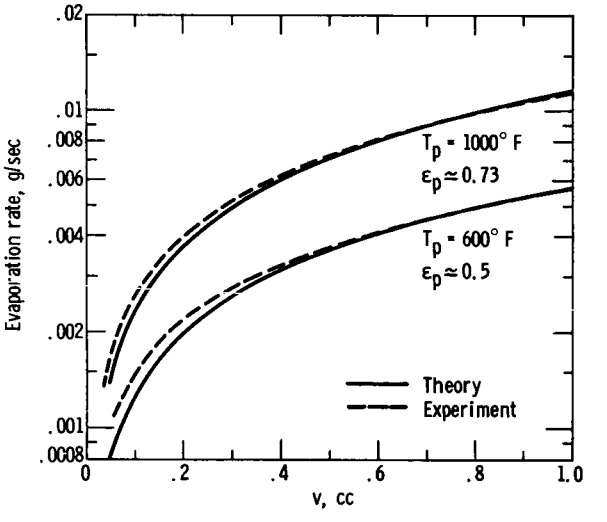

Figure 11. - Theoretical and experimental mass evaporation rates of water drops as a function of drop volume, plate temperatures, and plate emissivity.

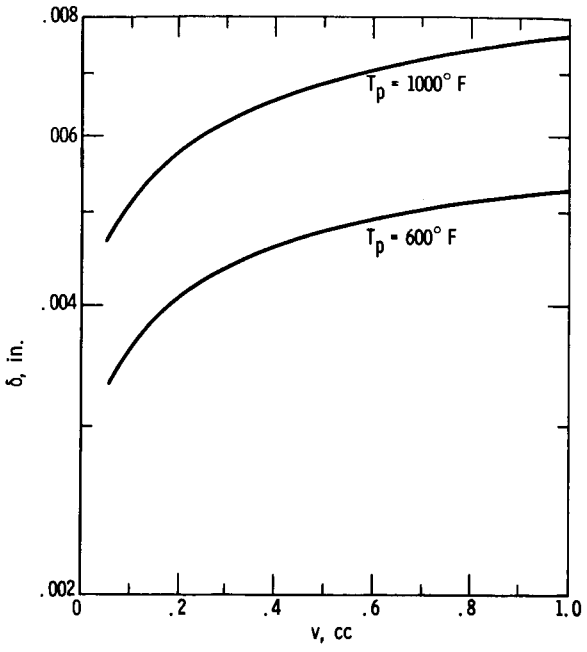

Figure 12. - Gap thickness of the water drop as a function of volume for plate temperatures of 600° and 1000° F and a plate emissivity of 0.5.

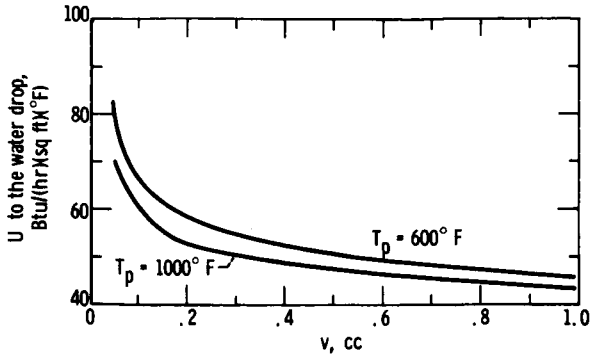

Figure 13. - Theoretical heat-transfer coefficient to the water drop as a function of volume for plate temperatures of 600° and 1000° F and a plate emissivity of 0.5.

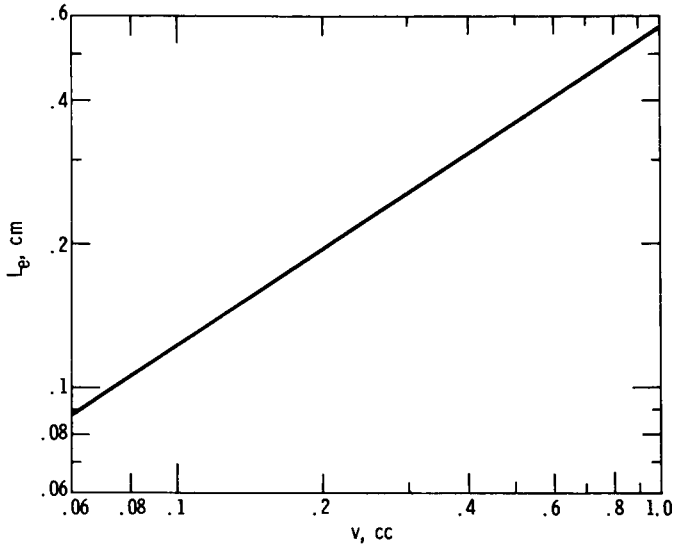

Figure 14. - Effective geometry factor L_e as a function of drop volume for water for an acceleration of 32.2 ft/sec^2.

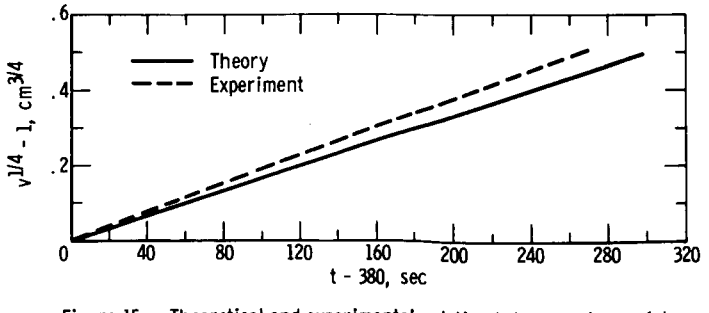

Figure 15. - Theoretical and experimental relation between volume of drop and vaporization time for water for volumes from 1 to 5 cc with a plate temperature of approximately 600° F.